Electromechanical response of ionic polymer-metal composites

Sia Nemat-Nasser[a] and Jiang Yu Li
Center of Excellence for Advanced Materials, University of California, San Diego, La Jolla, California 92093-0416

(Received 14 June 1999; accepted for publication 3 December 1999)

An ionic polymer-metal composite (IPMC) consisting of a thin Nafion sheet, platinum plated on both faces, undergoes large bending motion when an electric field is applied across its thickness. Conversely, a voltage is produced across its faces when it is suddenly bent. A micromechanical model is developed which accounts for the coupled ion transport, electric field, and elastic deformation to predict the response of the IPMC, qualitatively and quantitatively. First, the basic three-dimensional coupled field equations are presented, and then the results are applied to predict the response of a thin sheet of an IPMC. Central to the theory is the recognition that the interaction between an imbalanced charge density and the backbone polymer can be presented by an eigenstress field (Nemat-Nasser and Hori, *Micromechanics, Overall Properties of Heterogeneous Materials*, 2nd Ed., Elsevier, Amsterdam, 1999). The constitutive parameter connecting the eigenstress to the charge density is calculated directly using a simple microstructural model for Nafion. The results are applied to predict the response of samples of IPMC, and good correlation with experimental data is obtained. Experiments show that the voltage induced by a sudden imposition of a curvature, is two orders of magnitude less than that required to produce the same curvature. The theory accurately predicts this result. The theory also shows the relative effects of different counter ions, e.g., sodium versus lithium, on the response of the composite to an applied voltage or a curvature. © *2000 American Institute of Physics.* [S0021-8979(00)09005-8]

I. INTRODUCTION

An ionic polymer-metal composite (IPMC) consisting of a thin Nafion membrane (178 μm thick) sandwiched between two thin platinum plates (less than 1 μm thick), has been processed by Millet *et al.*,[1] following a procedure developed by Takenaka *et al.*,[2] as a solid polymer electrolyte for water electrolysis, as well as for application to fuel-cell technology. The composite has excellent chemical and mechanical stability, high ionic conductivity, and gas impermeability. Its use as an electroactive polymer composite seems to have been realized in the early 1990's by Oguro *et al.*[3] in Japan, and by Sadeghipour *et al.*[4] and Shahinpoor[5] in the United States. A strip of this composite in a swollen wet condition undergoes large bending motion when an alternating electric field is applied across its thickness. Conversely, when the strip is suddenly bent, a voltage is produced across its faces. Gold-plated IPMCs, using perfluorocarboxylic acid membranes, with similar properties, have been produced recently by Sewa *et al.*[6]

The IPMCs are distributed ''soft'' sensors and actuators, capable of large deformations. They offer great opportunities for many biomechanical and biomimetical applications. The pioneer work of Kuhn and his colleagues[7,8] on mechanochemical engines showed that water-swollen macromolecules can convert chemical energy into mechanical energy. Since then significant progress has been made in the development of stimulus-responsive polymer gels which respond to the applied electric field, to changes in the *p*H, and to changes in the temperature.[9] Applications of electroactive polymer gels in artificial muscles, smart material systems, and microelectromechanical systems (MEMS) are currently being actively pursued by many investigators. One of the features of polymer gels is the slow response time which is of the order of 1–10 s, compared with 10^{-3}–10^{-2} s of living skeletal muscles. The time required for the reconfiguration of ions in a thin sheet of IPMC, on the other hand, is very short relative to the vibrational periods of most mechanical systems. Hence, the reaction time is solely controlled by the mechanical properties. Thus, the material is promising for those applications which require a quick response time. Another feature of an IPMC is that it functions as both a distributed actuator and sensor. This attribute could be tailored at the molecular level to produce different responses to different stimuli, making it an attractive system for certain applications.

While these novel smart composites have many potential applications, the mechanisms which control their macroscopic behavior have not been fully understood. This article is a step toward remedying this paucity. As a starting point, the fundamental field equations which govern the response of the material are systematically developed. It is hoped that such an approach would encourage further modeling which would enable the polymer chemists to optimize the material at the molecular level, to design new materials and devices, and to further understand other chemomechanical and biologic systems. In this article, we outline a set of field equations which characterize the electrochemomechanical response of this composite. For the sake of completeness, the coupled three-dimensional field equations are first presented. Then the results are simplified for application to the bending of a strip of a Nafion-platinum composite. The basic field

[a]Electronic mail: sia@shiba.ucsd.edu

equations are solved for this special case and it is shown that the theory, both qualitatively and quantitatively, predicts the observed response of this composite, at least in a certain range of the applied potential or deformation. The constitutive parameters in the proposed model are estimated based on the microstructure of the composite, using micromechanics, or they are determined from the experiments. Central to the theory is the recognition that the internal stresses produced by the presence of electrically unbalanced negative ions that are permanently fixed to the backbone polymer, can be represented by an eigenstress.[10] The constitutive parameter connecting the eigenstress to the charge density is calculated directly using a simple microstructural model. The results are applied to predict the response of samples of IPMC, and good correlation with experimental data is obtained. In particular, the theory correctly predicts the observed results that a suddenly imposed curvature induces a voltage which is two orders of magnitude smaller than that necessary to produce the same curvature. The theory also shows the relative effects of different counter ions, e.g., sodium versus lithium, on the response of the composite to an applied voltage or a curvature.

This article is organized as follows. In Sec. II a brief account of the microstructure of the composite and the plating procedure is presented, based on the work of Millet *et al.*[1,11] The basic field equations are then presented in Sec. III. They are specialized for application to the bending motion of a strip of the composite in Sec. IV. In Sec. V, various constitutive parameters are calculated and numerical results are obtained and compared with experimental observations.

II. MATERIAL

Nafion, produced by DuPont de Nemours, is a copolymer of tetrafluoroethylene and sulfonyl fluoride vinyl ether, having the following chemical formula:

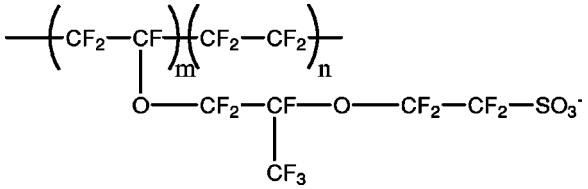

(1)

This linear fluorocarbon polymer, having some (no more than 10 mol %) pending acid groups, is strongly affected by water content and cations, because it combines two incompatible components, i.e., the hydrophobic fluorocarbon with the hydrophilic ionic phase, and has the phase-separation morphology of discrete hydrophobic and hydrophilic regions. The polytetrafluoroethylene in this material provides the three-dimensional structured backbone system, having regularly spaced long perfluorovinyl ether pendant side chains which terminate in ionic sulfonate groups. The ionic groups tend to aggregate to form tightly packed regions referred to as clusters,[12,13] which are fully interconnected and are readily saturated by water. The membrane is permeable to water and cations, while it is impermeable to anions.

The plating of the Nafion by micron-thick platinum metal is implemented from inside out, using an ingenious procedure developed by Takenaka *et al.*,[2] as described by Millet *et al.*[1,11] The Nafion is first ''cleaned'' by boiling it in 35% nitric acid for 30 min, then in deionized water for 1 h, to get rid of foreign materials. It is then immersed in a solution of platinum tetramine dichloride ($Pt[NH_3]_4Cl_2$) for a specific period, at room temperature, to incorporate the platinum salt into the membrane. Finally, the Pt^{++} is reduced to Pt metal by immersing in a suitable borohydride (MBH_4) for 2 h at room temperature, to reduce the platinum salt to platinum metal deposited on the membrane faces, where M may be lithium, sodium, potassium, or other elements of this group. The quality of the product critically depends on the concentration of the platinum salt and the incorporation period, as well as on the concentration of the reducing agent; using this procedure, the composite has been produced at UCSD. (This is an ongoing collaboration among the authors, Professor Yitzhak Tor, Dr. Masoud Beizai, and graduate student Phoebe Glazer.) When done properly, the micron-thick platinum becomes fully integrated with the Nafion membrane on both faces, providing the necessary electrodes. The platinum plate, as well as the Nafion layer, are microscopically porous. The mechanical response of the composite to an applied voltage, depends on the nature of the counter ions. We consider the cases where the counter ion in the Nafion is sodium, Na^+, or lithium, Li^+. Under wet conditions, this IPMC bends in an electric field, and produces a voltage when it is bent. Our aim is to provide a set of equations which may be used to predict these phenomena quantitatively. Explicit results are obtained and are compared with experimental data.

III. BASIC FIELD EQUATIONS

Figure 1(a) is a schematic representation of a model of the microstructure of water-saturated Nafion in the electrically neutral state. It shows the phase-separation morphology of discrete hydrophobic and hydrophilic regions, where the hydrophobic region is composed of the fluorocarbon polymer backbone, and the hydrophilic region contains the ionic groups and counter ions. In this model, the ionic groups are permanently attached to the fluorocarbon backbone, while the counter ions are free to move through the interstitial regions which are saturated with water. As a result of electrostatic interaction, the ionic groups in Nafion tend to aggregate to form tightly packed regions referred to as clusters.[12,13] Under an electric field, the cations are redistributed, resulting in a microscopic, locally imbalanced net charge density which produces internal stresses acting on the backbone polymer. As pointed out by Forsman,[14] the clustering of ionic groups in sulfonate ionomers is accompanied by an increase in the mean radius of gyration of the polymer chains. Thus, upon the redistribution of the cations, in the resulting anion-rich region, the polymer chains relax, while in the cation-rich region, they further extend, leading to the bending of the polymer membrane; see Fig. 1(b). In general, the redistribution of cations is accompanied by a redistribution of the water molecules which are carried by the cations. It is often suggested that this differential water distribution may produce differential swelling which may lead to the

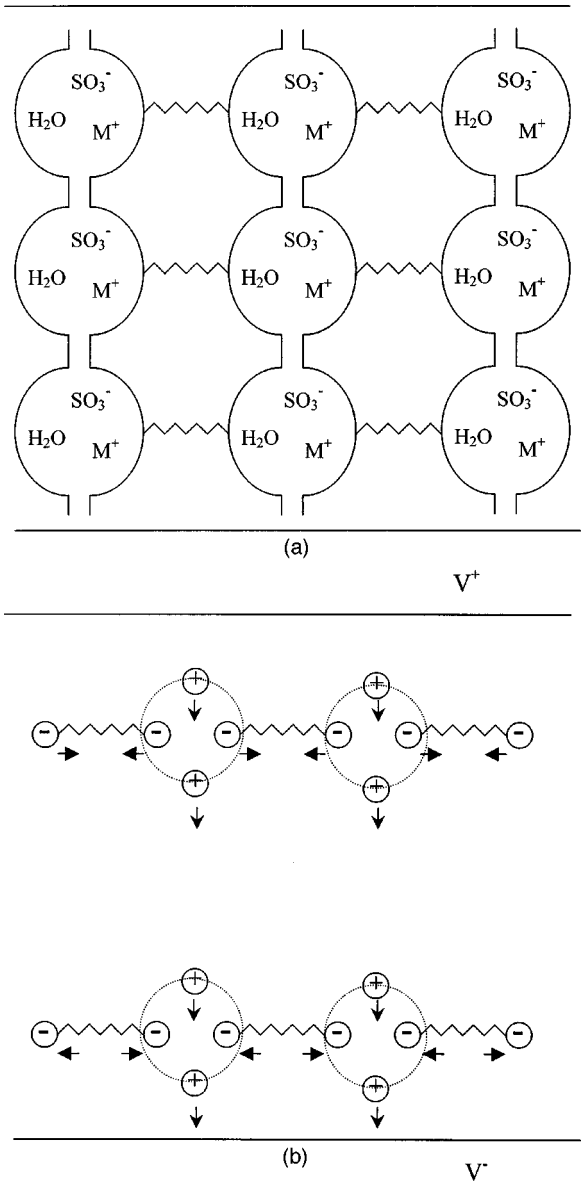

FIG. 1. Schematic representation of a possible microstructure for hydrated Nafion: (a) electrically neutral state with interconnected clusters, permeable to water and cations, and (b) in an electric field which redistributes the cations, leaving a net negative charge density near the anode and a net positive charge density near cathode.

bending deformation of the IPMC. While this mechanism may well dominate the deformation process for certain cases under certain ranges of boundary data, our analysis seems to suggest that the electrostatic forces must be dominant in the linearized model that we have developed to explain the quick response to a suddenly applied electric field. The resolution of the relative influence of electrostatic and fluid-induced swelling forces, and their coupling effects, requires a systematic experimental evaluation which is currently underway. Here, we shall focus on the electrostatically induced deformation of the IPMC. In the following development, the Nafion membrane is assumed to be isotropic, with permanently attached sulfonates uniformly distributed throughout the polymer. The results can be generalized to include anisotropy and heterogeneous distribution of sulfonates without any difficulty.

The stress field within the membrane is decomposed into an elastic part which is carried by the backbone polymer, denoted by $\boldsymbol{\sigma}$, and an eigenstress, $\boldsymbol{\sigma}^*$, which represents the effect of the imbalanced charge density, i.e.,

$$\boldsymbol{\sigma}^T = \boldsymbol{\sigma} + \boldsymbol{\sigma}^* \quad (\text{in V}), \tag{2}$$

where $\boldsymbol{\sigma}^T$ is the total stress. We assume that the eigenstress is given by

$$\boldsymbol{\sigma}^* = \boldsymbol{\sigma}^e + \boldsymbol{\sigma}^o. \tag{3}$$

In Eq. (3), $\boldsymbol{\sigma}^e$ is the electrostatic stress due to the imbalanced charge density given by

$$\boldsymbol{\sigma}^e = -k_0 \rho \mathbf{1}, \quad \rho = (C^+ - C^-)F, \tag{4}$$

where k_0 is yet to be calculated, $\mathbf{1}$ is the identity tensor, ρ is the charge density, C^+ and C^- are the positive and negative ion densities (mol/m^3), respectively, and F is Faraday's constant (96,487C/mol). $\boldsymbol{\sigma}^o$ is the osmotic stress due to the redistribution of water molecules which are carried by the cations. We assume that the osmotic stress can be represented by

$$\boldsymbol{\sigma}^o = -\mathbf{C}_p \boldsymbol{\epsilon}^o, \tag{5}$$

where $\mathbf{C}_p$ is the elastic stiffness tensor of the swollen Nafion, and $\boldsymbol{\epsilon}^o$ is the volumetric strain due to the water redistribution. The eigenstress induced by other effects is assumed to be negligible, for the considered cases.

With $\mathbf{D}$, $\mathbf{E}$, and ϕ, respectively denoting the electric displacement, the electric field, and the electric potential, the charge distribution is governed by the following field equations:

$$\boldsymbol{\nabla} \cdot \mathbf{D} = \rho, \quad \mathbf{D} = \kappa_e \mathbf{E}, \quad \mathbf{E} = -\boldsymbol{\nabla} \phi, \tag{6}$$

where κ_e is the effective dielectric constant of the polymer. In view of Eqs. (4) and (6), the electrostatic stress is related to the electric field by

$$\boldsymbol{\sigma}^e = -k_0 \boldsymbol{\nabla} \cdot (\kappa_e \mathbf{E}) \mathbf{1}. \tag{7}$$

Since the anions are assumed to be permanently attached to the backbone structure, having a uniform distribution, it follows that $\boldsymbol{\nabla} C^- = 0$. Hence,

$$\boldsymbol{\nabla} C^+ = \frac{1}{F} \boldsymbol{\nabla} [\boldsymbol{\nabla} \cdot (\kappa_e \mathbf{E})] = -\frac{\kappa_e}{F} \boldsymbol{\nabla} (\nabla^2 \phi), \tag{8}$$

if we assume that κ_e is constant.

The distribution of the counterions is governed by the continuity equation,

$$\frac{\partial C^+}{\partial t} + \boldsymbol{\nabla} \cdot \mathbf{J} = 0, \tag{9}$$

where t measures time, and $\mathbf{J}$ is the ion flux vector, given by[15]

$$\mathbf{J} = -d \left(\boldsymbol{\nabla} C^+ + \frac{C^+ F}{RT} \boldsymbol{\nabla} \phi + \frac{C^+ \Delta V}{RT} \boldsymbol{\nabla} p \right) + C^+ \mathbf{v}; \tag{10}$$

here d is the ionic diffusivity, R is the gas constant, T is the absolute temperature, p is the fluid pressure, and

$$\Delta V = M^+\left(\frac{V^+}{M^+} - \frac{V^w}{M^w}\right), \tag{11}$$

in which V^+ and V^w are partial molar volumes of the cation and water, respectively, and M^+ and M^w are the corresponding molar weights. In Eq. (10), $\mathbf{v}$ is the free water velocity field. In the present model, we assume that it is given by Darcy's law,[16,17]

$$\mathbf{v} = d_h(-C^- F\nabla\phi - \nabla p), \tag{12}$$

where d_h is the hydraulic permeability coefficient.

Finally, dynamic equilibrium requires that

$$\nabla\cdot\boldsymbol{\sigma}^T = \rho_0\frac{d\mathbf{V}}{dt} \quad (\text{in V}), \tag{13}$$

with all three stress fields, $\boldsymbol{\sigma}^T$, $\boldsymbol{\sigma}$, and $\boldsymbol{\sigma}^*$, being symmetric second-order tensors. In Eq. (13), ρ_0 is the mass density and $\mathbf{V}$ is the velocity of the IPMC when viewed as a continuum. Equations (2)–(13) are the field equations defining the response of the ionic polymer in an electric field. They must be supplemented with appropriate boundary and initial conditions for specific applications, as well as with constitutive relations for the polymer.

When the applied electric field is time independent and no external load is applied to the composite, at the equilibrium state, the distribution of the cations is obtained from

$$\mathbf{J} = \mathbf{0}, \quad \mathbf{v} = \mathbf{0} \quad (\text{in V}). \tag{14}$$

From Eqs. (10) and (12) we now have

$$\frac{\kappa_e}{F}\nabla(\nabla\cdot\mathbf{E}) - \frac{\kappa_e}{RT}(\nabla\cdot\mathbf{E})\mathbf{E}(1-C^-\Delta V) - \frac{C^- F}{RT}(1-C^-\Delta V)\mathbf{E} = 0, \tag{15}$$

where Eqs. (6) and (8) are also used. We assume here that $(\kappa_e/RT)\nabla\cdot\mathbf{E} \ll (C^- F/RT)$, i.e., we neglect the nonlinear term and reduce Eq. (15) to

$$\nabla(\nabla\cdot\mathbf{E}) - \frac{C^- F^2}{\kappa_e RT}(1-C^-\Delta V)\mathbf{E} = 0, \tag{16}$$

which is the final equation of this linearized model, to be integrated subject to given boundary conditions. From the solution we obtain later, it is found that this assumption is valid almost everywhere within the membrane. Once the electric field $\mathbf{E}$ is obtained, the electrostatic eigenstress $\boldsymbol{\sigma}^e$ is calculated, using Eq. (7). In this quasi-static case, the stress field in the polymer is then obtained from

$$\nabla\cdot\boldsymbol{\sigma} = -\nabla\cdot\boldsymbol{\sigma}^* = \frac{k_0 C^- F^2}{RT}(1-C^-\Delta V)\mathbf{E} - \nabla\cdot\boldsymbol{\sigma}^o \quad (\text{in V}), \tag{17}$$

which must be integrated, together with given stress- or displacement-boundary conditions. We assume that linear elasticity constitutive relations may be used to relate the stress, $\boldsymbol{\sigma}$, to the strain, $\boldsymbol{\epsilon}$, in the polymer, i.e.,

$$\boldsymbol{\sigma} = \mathbf{C}_p : \boldsymbol{\epsilon}, \quad \boldsymbol{\epsilon} = \tfrac{1}{2}[\nabla\mathbf{u} + (\nabla\mathbf{u})^T], \tag{18}$$

where $\mathbf{u}$ is the displacement field; see, e.g., Nemat-Nasser and Hori[10] for more details.

It is still necessary to calculate the constitutive parameter, k_0 of Eq. (4). To this end, we must take into account the detailed microstructure of Nafion. It is widely accepted that the ionic groups in Nafion tend to aggregate to form tightly packed regions referred to as clusters. The clustering phenomenon has been supported by both theoretical[12,18] and experimental observations.[13,19,20] Readers are referred to review articles by Mauritz[21] and Heitner-Wirguin[22] for details. Although the detailed microstructural arrangement of clusters is yet to be determined, for modeling purposes, the clusters may be represented by spheres of radii ranging from 20 to 50 Å. For our modeling, we assume that all the anion-cation pairs are distributed on the spherical surface of the clusters, inside which there is a continuous body of water. In the absence of an applied electric field, the net charge inside each cluster is zero. We consider the electrostatic interaction between ion pairs inside a cluster, ignoring the interaction between different clusters. Every anion attached to a fluorocarbon polymer chain is equilibrated by two competing forces: one is due to the electrostatic interaction with other ions in the cluster, F_i, and the other is due to the elastic interaction with the polymer chain, F_e, so that

$$F_i + F_e = 0. \tag{19}$$

Upon the application of a voltage at the boundary, the cations are redistributed, changing the electrostatic interaction among the ion pairs. In the new equilibrium state,

$$\Delta F_i + \Delta F_e = 0, \tag{20}$$

where ΔF is the corresponding change in the interaction force; ΔF_i is the source that produces the eigenstress. The redistribution of cations introduces a net effective charge inside the cluster, located at the center of the cluster, due to symmetry. The electrostatic interaction of individual anions with their ionic environment has two components, one is due to the interaction with other ion pairs, which, to a first order of approximation, will not change with the introduction of the net effective charge, and the other is due to the net effective charge introduced at the cluster center. Therefore, the change in the electrostatic interaction force ΔF_i, may be estimated, according to Coulomb's law, as follows:

$$\Delta F_i = \frac{-e}{4\pi\kappa_e r_c^2}(C^+ - C^-)F r_d^3, \tag{21}$$

where r_c is the cluster radius, r_d is the mean distance between clusters, and e is the elementary charge (1.6×10^{-19} C); see Fig. 2(a). The charge density inside the cluster is larger than the average charge density $(C^+ - C^-)F$, because it is assumed that all ions are located inside the clusters. From Eqs. (20), (21), and (4), we have

$$k_0 = \frac{e}{4\pi\kappa_e r_c^2}\frac{r_d^3}{\pi r_e^2}, \tag{22}$$

where r_e is the effective radius of the polymer chain. It is clear that the internal stress induced by the charge redistribution is isotropic, due to the spherical geometry. Equation

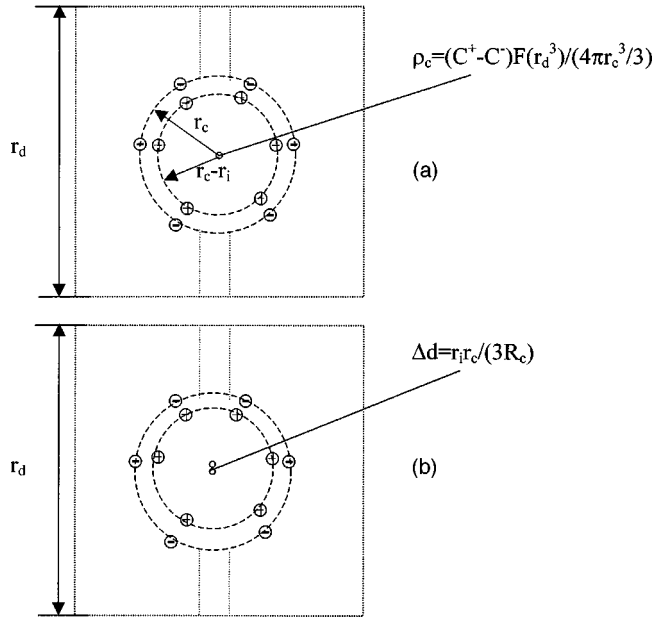

FIG. 2. Schematic representation of Nafion membrane:(a) internal stresses induced by interaction between ion pairs inside a cluster, and (b) dipole induced by imposed bending curvature.

(22) shows how the geometric parameters defining the microstructure of the polymer, affect the magnitude of the force which can be induced in the composite by an electric field; see also Eqs. (4) and (17). The cluster radius r_c and the cluster spacing r_d can be modified by changing the length and density of the side chains which carry the sulfonates. (The Dow Chemical Company has developed a perfluorinated ionomer with shorter side chains than those of Nafion.) Thus, it may be possible to tailor the microstructure for an optimal response.

IV. RESPONSE OF THIN STRIP OF IPMC

A platinum-plated strip of Nafion in a swollen water-saturated state, is approximately 200 μm thick. Denote the thickness by $2h$, and let x measure the distance along the thickness, from the midplane of the strip; see Fig. 3. Assume that the face $x=h$ is grounded, so that $\phi(h)=0$, and the other face carries a uniform potential, $\phi(-h)=\phi_0$. All field quantities are now functions of x and t only. It will be shown at the end of this section that the time required for the cations to redistribute themselves over the thickness of the strip, is very small based on the present formulation. Hence, if the applied potential, ϕ_0, is alternating with a frequency of several Hz, the redistribution of ions and hence the ionic response can be assumed to be essentially instantaneous. This may not, however, be the case when other effects, such as swelling due to osmotic pressure, are considered.

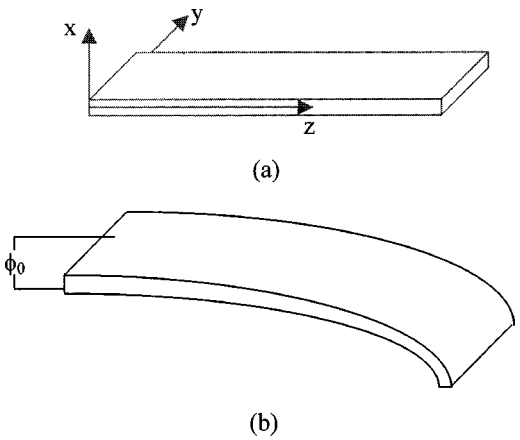

FIG. 3. Schematic diagram of a thin strip of IPMC: (a) in electrically neutral state, and (b) being bent in an applied electric field.

A. Deformation due to applied potential

In view of the above comments, Eq. (16) which, in the present case, takes on the form

$$\frac{\partial^2 E_x}{\partial x^2}-a^2E_x=0,\quad a^2=\frac{C^-F^2}{\kappa_e RT}(1-C^-\Delta V)\doteq\frac{C^-F^2}{\kappa_e RT}, \tag{23}$$

is used, even if the applied potential ϕ_0 is time dependent. The last estimate in Eq. (23) is based on the fact that $|C^-\Delta V|\ll 1$. In what follows, the subscript x or z is used to denote vector or tensor components in the x or z direction. Using $\partial\phi(x)/\partial x=-E_x$, the boundary conditions, $\phi(-h)=\phi_0$ and $\phi(h)=0$, and $\int_{-h}^{h}\rho dx=0$, the following expressions are obtained:

$$\begin{aligned}
\phi&=-\frac{\phi_0}{2\sinh(ah)}\sinh(ax)+\frac{\phi_0}{2},\\
E_x&=\frac{\phi_0 a}{2\sinh(ah)}\cosh(ax),\\
\sigma^e_{zz}&=\sigma^e_{yy}=-\frac{k_0\kappa_e\phi_0 a^2}{2\sinh(ah)}\sinh(ax),\\
C^+&=C^-+\frac{\kappa_e\phi_0 a^2}{2F\sinh(ah)}\sinh(ax).
\end{aligned} \tag{24}$$

When no external loads are applied, $\sigma^T_{zz}=\sigma^T_{yy}=0$, and therefore, $\sigma_{zz}=\sigma_{yy}=-\sigma^e_{zz}$. We have ignored the osmotic stress $\boldsymbol{\sigma}^o$ here, assuming that it is small compared with the electrostatic stresses; this will be discussed in the next section. In general, the osmotic stress can be estimated from the water distribution inside the Nafion membrane, which is closely related to the cation distribution. The stresses, $\sigma_{zz}=\sigma_{yy}$, act normal to the planes of the cross section, in the z and y directions, creating out-of-plane bending of the strip. If the strip is long in the z direction and narrow in the y direction, as shown in Fig. 3(a) then the bending occurs as suggested in Fig. 3(b). The resulting bending moment and the corresponding curvature are given by

$$\begin{aligned}
M&=\int_{-w/2}^{w/2}\int_{-h}^{h}x\sigma_{zz}dxdy\\
&=\frac{k_0\kappa_e\phi_0 a}{\sinh(ah)}\left[h\cosh(ah)-\frac{\sinh(ah)}{a}\right]w\doteq k_0\kappa_e\phi_0 ahw,\\
R_c&=\frac{\overline{Y}I}{M}=\frac{2\overline{Y}h^2}{3k_0\kappa_e\phi_0 a},
\end{aligned} \tag{25}$$

where w is the width of the membrane, $\overline{Y}$ is the effective Young modulus of the composite, and I is the cross-sectional moment of inertia. Since the bending moment is constant along the length, so is the curvature.

It is worthwhile to examine the solution given by Eqs. (24). In the present linearized approximation, the magnitude of a is of the order of 10^{10}, the charge density ρ being virtually zero everywhere inside the membrane. Under these conditions, it is indeed verified that the nonlinear term in Eq. (15) is negligible. Near the boundaries of the membranes, i.e., at $x=\pm h$, the solution suggests the presence of a thin boundary layer, within which most of the imbalanced charges are distributed. Since the maximum negative charge density cannot exceed C^-F, we calculate the total charge within half of the membrane to estimate the thickness of this boundary layer. The total imbalanced charge per unit length is

$$Q=w\int_0^h (C^+-C^-)F\,dx=\frac{a\kappa_e\phi_0 w}{2}\tanh(ah/2)\doteq\frac{a\kappa_e\phi_0 w}{2}. \tag{26}$$

If these charges are assumed to be all distributed within a thin boundary layer at the surface, with the maximum possible charge density of C^-F, the thickness of the boundary layer would be

$$l=\frac{Q}{wC^-F}=\frac{a\kappa_e\phi_0}{2C^-F}. \tag{27}$$

Such a charge distribution will induce the following electrostatic stress over the length l:

$$\sigma^e_{zz}=\sigma^e_{yy}=-k_0C^-F, \tag{28}$$

which gives a bending moment

$$M=2\int_{-w/2}^{w/2}\int_{h-1}^{h} x(-\sigma^e_{zz})\,dx\,dy\doteq k_0\kappa_e\phi_0 ahw, \tag{29}$$

which is equivalent to Eq. (25). Thus by introducing a thin boundary layer, in which charges are uniformly distributed, we obtain the same bending moment as given by Eq. (25), while overcoming the difficulty presented by the linearized solution, Eq. (24). The charge density, however, may not have the maximum value, C^-F. Any uniformly distributed charge density within a thin boundary layer, equivalent to the total charge Q, yields the bending moment given by Eq. (29), as long as the boundary layer thickness l is small enough compared with h so that $2h-l\doteq 2h$.

B. Potential due to imposed deformation

If instead of an applied electric field, the strip is suddenly bent by the application of a bending moment which produces a stress, $\boldsymbol{\sigma}$, on the backbone polymer, then an electric potential is generated across the composite, due to the differential displacement of the effective centers of the anions and cations within each cluster, producing an effective dipole. Since this differential displacement is second order in magnitude, the resulting electric potential will also be a second-order quantity. The displacement along the x axis of the membrane subjected to an applied bending curvature is given by[23]

$$u_x=\frac{z^2+\nu x^2-\nu y^2}{2R_c}, \tag{30}$$

where ν is the Poisson ratio of the membrane and R_c is the imposed radius of curvature. This imposed displacement field distorts the ionic clusters, creating an effective dipole within each cluster. To estimate the value of this dipole, consider a spherical cluster of radius r_c, with center at $(x_\alpha,0,0)$, and assume that the fixed anions are uniformly distributed on the surface of this sphere, while the cations are uniformly distributed over a sphere of the same center but of radius r_c-r_i, where r_i is the distance between the anion and cation in an ion pair; see Fig. 2(a). The distributed charges are equivalent to an effective total charge located at the common center of the two spheres prior to the applied distortion, producing zero total charge and dipole. The imposed deformation displaces the effective anion and cation charge centers by different amounts, producing an effective dipole; see Fig. 2(b). The displacement of the effective charge center is estimated by averaging the resulting surface displacement over each surface. For a typical αth sphere of radius r_c and center at $(x_\alpha,0,0)$, the effective charge center moves by the distance

$$\Delta u_x(x_\alpha)=\frac{1}{2R_c}\frac{1}{4\pi r_c^2}\int_0^\pi\int_0^{2\pi}[r_c^2\sin^2\theta(\cos^2\psi-\nu\sin^2\psi)+\nu(r_c\cos\theta+x_\alpha)^2]r_c^2\sin\theta\,d\psi\,d\theta=\frac{r_c^2+3\nu x_\alpha^2}{6R_c}, \tag{31}$$

where the spherical coordinate system is used. The separation of the effective centers of anions and cations in a cluster, due to the imposed bending curvature, denoted by $\Delta d(x_\alpha)$ for the αth cluster, is now given by

$$\Delta d(x_\alpha)=\frac{1}{6R_c}[r_c^2-(r_c-r_i)^2]\doteq\frac{r_ir_c}{3R_c}, \tag{32}$$

which is independent of x_α. The separation of the effective charge centers introduces a dipole $\boldsymbol{\mu}$ in the cluster, which induces a potential field. The magnitudes of the dipole, μ, and the resulting potential, ϕ_α, are given by[24]

$$\mu(x_\alpha)=q_{\text{total}}\Delta d=C^-Fr_d^3\frac{r_ir_c}{3R_c},\quad \phi_\alpha=\frac{q_{\text{total}}}{4\pi\kappa_w r}+\frac{\boldsymbol{\mu}\cdot\mathbf{r}}{4\pi\kappa_w r^3}, \tag{33}$$

where q_{total} is the total positive charge inside the cluster, $\mathbf{r}$ is the position vector of magnitude r with respect to the induced dipole, and κ_w is the dielectric constant of water $(78\kappa_0)$. Now, we have a series of clusters of water embedded in the polymer backbone, each with a dipole at its center. The electric field at $\mathbf{r}$ in the polymer, $\mathbf{E}(\mathbf{r})$, induced by the dipole, $\boldsymbol{\mu}$, located at the cluster center, is given by

$$\mathbf{E}(\mathbf{r})=-\frac{1}{4\pi\kappa_w}\frac{3}{2\kappa_p/\kappa_w+1}\left[\frac{\boldsymbol{\mu}}{r^3}-\frac{3(\boldsymbol{\mu}\cdot\mathbf{r})\mathbf{r}}{r^5}\right], \tag{34}$$

TABLE I. Water absorption of Nafion in Li^+ Na^+ salt forms.[a,b]

Cation	ρ_d (10^3 kg/m^3)	δm (%)	δV (%)	C^- (mol/m^3)	C^W (mol/m^3)	κ_e/κ_0	a (10^9)
Li^+	2.078	29.7	61.7	1070	21300	6.10	8.60
Na^+	2.113	21.0	44.3	1200	17100	5.27	9.80

[a]Gierke *et al.*, 1981.
[b]Narebska *et al.*, 1985.

where κ_p is the dielectric constant of polymer ($3\kappa_0$). The derivation of Eq. (34) is given in Appendix A. We will use the electric field on the boundary between two clusters as the average electric field in the membrane, which is the sum of the contributions from all the dipoles along the thickness direction,

$$E=2\sum_{n=0}^{n=\infty}\frac{1}{(2n+1)^3}\frac{1}{4\pi\kappa_w}\frac{3}{2\kappa_p/\kappa_w+1}\frac{2\mu}{(r_d/2)^3}, \tag{35}$$

where E is the magnitude of the resulting electric field. This leads to a potential difference across the thickness, given by

$$\Delta\phi=2hE. \tag{36}$$

C. Estimate of charge-relaxation time

Finally, we estimate the relaxation time for the redistribution of the positive charges when the applied electric field is suddenly changed, by considering the continuity Eq. (9) which, with the aid of the other field equations and linearization, can be reduced to

$$\frac{\partial^3\phi}{\partial x^2\partial t}=d\left(\frac{\partial^4\phi}{\partial x^4}-a^2\frac{\partial^2\phi}{\partial x^2}\right). \tag{37}$$

Using the standard separation of variables, it is readily shown that the n-th relaxation time is given by

$$\tau_n=\frac{1}{\lambda_n},\quad \lambda_n=\left(\frac{n^2\pi^2}{h^2}+a^2\right)d. \tag{38}$$

Hence, the smallest relaxation time, τ_1, satisfies

$$\tau_1<\frac{1}{a^2d} \tag{39}$$

which is less than 10^{-12} s, as will be shown in the following section.

V. NUMERICAL RESULTS AND COMPARISON WITH EXPERIMENTS

A. Numerical estimate of parameters

From the results of the preceding section, it is clear that the cluster size is an important microstructural parameter that determines the response of IPMCs. It is related to the water absorption of the ionic polymer, here Nafion, which is listed in Table I for Li^+ and Na^+; in this table, ρ_d is the density of the dry membrane, and δm and δV are the fractional increments of weight and volume due to the water absorption.[13] The molar concentration of water may then be determined from

$$C^w=\frac{\rho_d\delta_m}{M^w(1+\delta V)}, \tag{40}$$

where M^w is the molar weight of water. From Narebska *et al.*,[25] the anion concentration in water-swollen Nafion of Na^+ salt is 1200 mol/m^3. Thus, the corresponding anion concentration of Li^+ is determined from

$$C^-_{\rm dry}=c^-_{\rm wet}(1+\delta V), \tag{41}$$

where $C^-_{\rm dry}$ and $C^-_{\rm wet}$ are the anion concentration in dry and wet Nafion membranes, respectively. These values are also listed in Table I. Now we can estimate the relative magnitude of the osmotic stress. Every anion is associated with 14 or 19 water molecules for Na^+ or Li^+ exchanged Nafion, according to Table I. Assuming every cation carries 4 water molecules with it, which is the hydration number for Na^+ (Ref. 26), it follows that the osmotic strain is proportional to $(C^+-C^-)/C^-(4/14)$. On the other hand, the electrostatic stress is proportional to $k_0(C^+-C^-)F$. So for the same ion-distribution profile, osmotic stress is orders of magnitude less than the electrostatic stress.

An interesting experimental observation, relating to the osmotic and electrostatic forces, is the difference in the response of the IPMC in air and in water. Upon the application of a step voltage to an IPMC in the dry air, the sample quickly bends towards the anode side, to a maximum position, and stays there, showing little tendency toward immediately returning to its neutral position. However, when the same step voltage is applied while the IPMC is immersed in water, the sample slowly relaxes backward toward its neutral initial position. The long-term response of the IPMC in water appears to involve several time-scales, as is also suggested by the experimental results reported by Kanno *et al.* (1996);[27] see their Fig. 3. In the present case, where a step voltage is applied to the water-saturated IPMC in air [Fig. 4(a)] and then held at a constant value for 6 s [Fig. 4(b)], before it is reversed [Fig. 4(c)], no relaxation toward the neutral position of Fig. 4(a), was displayed by the IPMC strip. On the other hand, when the same test is performed in water, relaxation toward the neutral position is observed during the 6 s, while a constant voltage exists across the strip. Hence, there are at least two effective time scales defining the short-time (less than 6 s) response of the strip: one is the initial (fast) response time, controlled by the electrostatic effects; and the other (slow relaxation response), occurring in the presence of water due to an osmotic process.

B. Effective properties

With virtually all the water inside the clusters (except for a small amount which is present in the channels connecting the clusters), the mean distance between adjacent clusters, r_d, is given as a function of the cluster radius, r_c, and the volume fraction of water, c, by

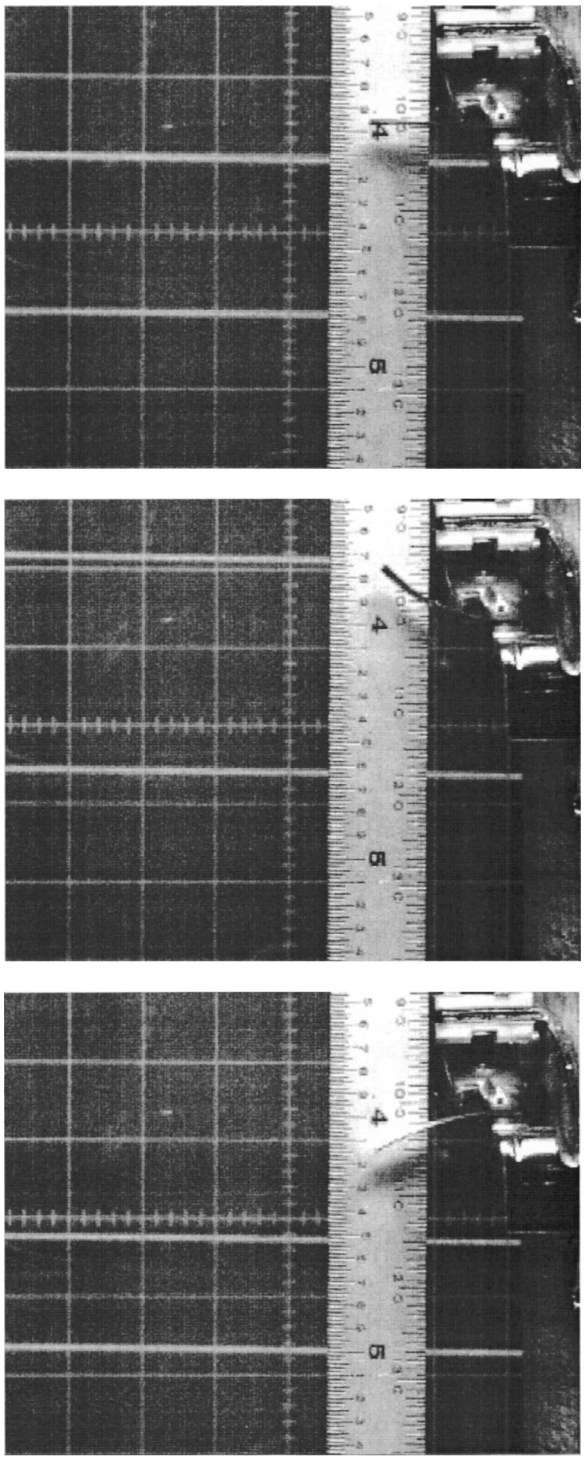

FIG. 4. Video frames of IPMC strip bending in an electric field: (a) in electrically neutral state, (b) bent upward, and (c) bent downward.

$$r_d=\left(\frac{4/3\pi r_c^3}{c}\right)^{1/3},\quad c=\frac{\delta V}{1+\delta V}. \tag{42}$$

The number of anions and water molecules per cluster, n_i and n_w, is then given by

$$n_i=r_d^3NC^-,\quad n_w=f\times n_i,\quad f=\frac{C^w}{C^-}. \tag{43}$$

where f is the molar ratio of water relative to the cations, and N is Avogadro's number (6.02×10^{23}). In Table II, we list the microstructural parameters for different cluster sizes, and the corresponding expected response of the IPMC strip. In the calculation, the effective dielectric constant of the IPMC is evaluated as

$$\kappa_e=\frac{2\kappa_p+\kappa_w-c(\kappa_p-\kappa_w)}{2\kappa_p+\kappa_w+c(\kappa_p-\kappa_w)}\kappa_p. \tag{44}$$

The derivation of Eq. (44) is given in Appendix B. The effective radius of the fluorocarbon polymer chain is assumed to be 2 Å (covalent radii of carbon and fluorine are 0.77 and 0.71 Å, respectively). The effective Young modulus of the composite is determined as follows. Defining the effective Young modulus $\overline{Y}$ of the IPMC strip by

$$\overline{Y}\int_{-h}^{h}x^2dx\,dy=\int_{-h}^{h}Y(x)x^2dx\,dy, \tag{45}$$

its estimated value is then 2.38 GPa, where the Young modulus of platinum is 146.8 GPa, while that of the hydrated Nafion is 0.23 GPa, measured by a three-point bending test; the total thickness of the IPMC is 203 μm, and the thickness of the platinum is about 0.5 μm. However, the measured Young modulus of the IPMC strip, obtained by the same three-point bending test, ranges from 0.5 to 0.65 GPa. The reduction in the effective modulus is due to the presence of microcracks in the platinum plates which are microscopically porous. With these parameters, the estimated relaxation time for the distribution of the cations is of the order of 10^{-12} s, as was mentioned before.

Table II provides a comparison between IPMCs exchanged by Na^+ and Li^+, for the same cluster size. Such a comparison needs further experimental justification. First, the cluster size and anion per cluster could be different for Na^+ and Li^+. Second, due to the difference in the water absorption, the corresponding Young modulus for the swollen Nafion would also be different.[18] All these effects influence the response of the IPMC strip. These effects are not included in the estimates given in Table II.

TABLE II. Microstructural and physical parameters of Nafion in Li^+ Na^+ salt forms corresponding to different cluster sizes.

Cation	Li^+ ($C^-=1070$ mol/m^3, $C^W=21300$ mol/m^3)					Na^+ ($C^-=1200$ mol/m^3, $C^W=17100$ mol/m^3)				
r_c (Å)	r_d (Å)	n_i	k_0 (J/C)	$R_c\,\phi_0$	$\Delta\phi\,R_c(10^{-6})$	r_d (Å)	n_i	k_0 (J/C)	$R_c\,\phi_0$	$\Delta\phi\,R_c(10^{-6})$
10	22.2	7	21	0.46	50.6	23.8	10	30	0.33	45.4
20	44.4	56	41	0.23	101	47.8	79	59	0.17	10.8
30	66.7	191	62	0.16	152	71.7	266	89	0.11	136
40	88.9	452	82	0.12	203	95.6	630	119	0.083	182
50	111	884	103	0.09	254	119	1232	148	0.066	227

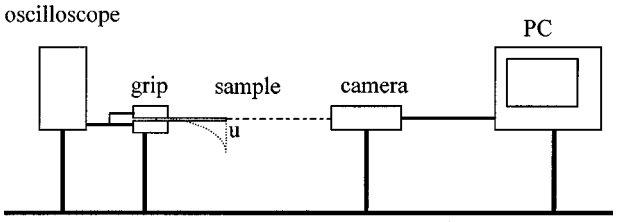

FIG. 5. Schematic diagram of experimental setup.

C. Comparison with experimental data

To verify whether the theoretical predictions based on the proposed model, are reasonable, we have measured the tip displacement $u = 2R_c \sin^2(l/2R_c)$ of various IPMC strips under a sinusoidal voltage. The schematic of the experimental setup is shown in Fig. 5. The sample is held in a grip through which the voltage is applied. Both the voltage and the current across the sample are displayed on an oscilloscope. A high-speed camera is used to video tape the tip displacement, the voltage, and the current on the oscilloscope. These are captured at the rate of 5 frames per second in an IBM PC by Bigpicture Asymetrix DVP Capture. The video clip is analyzed by a UTHSCSA ImageTool from which the digitized displacement, voltage, and current are obtained. The temperature is 300 K. The amplitude and frequency of the applied voltage are 2.5 V and 0.32 Hz, respectively.

Figure 6 shows the tip displacement of the strip versus time, and Fig. 7 shows the tip displacement of the strip as a function of the strip length. Other than a small difference in phase, good agreement between the predictions and measurements is observed. This difference in phase is due to the inertia and damping effects which have been ignored. It can actually be used to estimate the effective damping of the strip. Figure 8 shows the tip displacement of the IPMC versus the applied voltage; the experimental data are from Shahinpoor *et al.*[28] Figure 9 shows the predicted and measured voltage which is produced by suddenly bending a strip; the experimental data are from Mojarrad and Shahinpoor.[29] Again, good agreement is observed. In the calculations, the

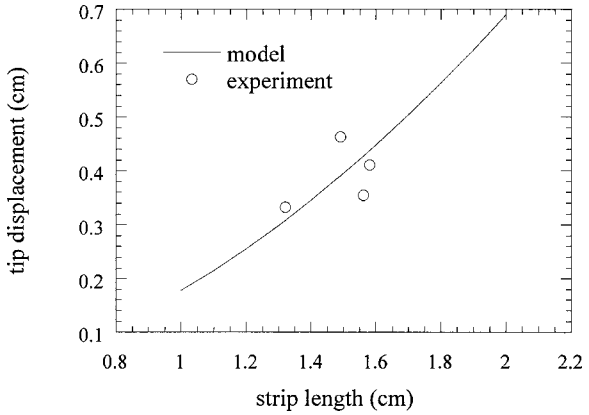

FIG. 7. Maximum tip displacement of IPMC strip vs strip length when a sinusoidal voltage is applied; Young modulus is 0.65 GPa.

cluster size is assumed to be 50 Å, and r_i is taken as 6 Å, which is approximately the sum of the radii of M^+ and SO_3^- and the diameter of one water molecule.

VI. CONCLUSIONS

A micromechanical theory is developed to explain the observed (short time, of the order of seconds) response of a water-saturated ionic polymer-metal composite (in air), i.e., bending under an applied electric field, and producing voltage when bent. The theory couples the ion transport, electric field, and elastic deformation to successfully predict the short-time response in air, qualitatively and quantitatively. The constitutive parameters are estimated based on the microstructure and composition of the membrane. These estimates provide guidance for tailoring the microstructure in order to obtain optimal desired macroscopic responses. They also suggest various experiments which can be used to verify the theoretical predictions and fine-tune the micromechanical model.

ACKNOWLEDGMENTS

The authors would like to thank Professor Shahinpoor for providing IPMC samples for our experiments. Useful discussions with Mr. Santosh Putta are gratefully acknowledged. The work reported here has been supported in part by

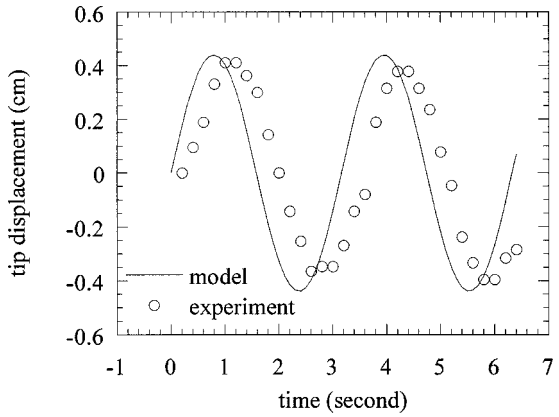

FIG. 6. Tip displacement of IPMC strip vs time when a sinusoidal voltage is applied; the sample length is 1.57 cm. Young modulus is 0.65 GPa.

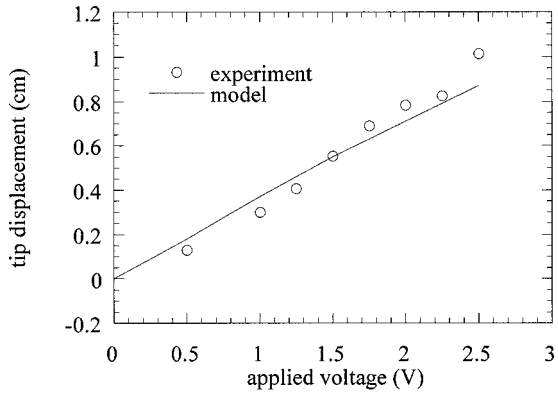

FIG. 8. Tip displacement of IPMC strip vs the applied voltage; Young modulus is 0.5 GPa; experimental data are from Ref. 28.

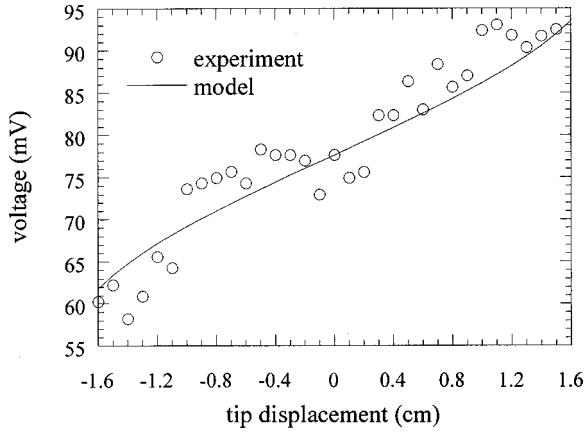

FIG. 9. Voltage produced by sudden bending at constant curvature vs the tip displacement of the IPMC strip; the effective sample length is 2.5 cm; experimental data are from Ref. 4.

Defense Advanced Projects Agency (DARPA, Dr. Steve Wax, Program Manager) and in part by the UCSD-endowed John Dove Isaacs Chair in Natural Philosophy.

APPENDIX A: ELECTRIC FIELD OF A DIPOLE

Consider a dipole $\boldsymbol{\mu}$ situated at the center of a spherical cluster which contains a continuous body of water inside, and is embedded in a polymer-backbone continuum. The general solution of Laplace's equation for the axially symmetric field is[30]

$$\Phi=\sum_{l=0}^{\infty}\left[a_l r^l+\frac{b_l}{r^{l+1}}P_l(\cos\theta)\right], \tag{A1}$$

where $P_l(\cos\theta)$ is the Legendre function, and θ measures the angle from the axis of symmetry (i.e., the dipole axis), and r measures the length from the origin. We denote the potential outside the cluster by ϕ_1, and that inside the cluster by ϕ_2. The boundary conditions are

$$\begin{aligned}&(\phi_1)_{r\to\infty}=0,\\ &(\phi_1)_{r=r_c}=(\phi_2)_{r=r_c},\\ &\kappa_p(\phi_1)'_{r=r_c}=\kappa_w(\phi_2)'_{r=r_c},\\ &(\phi_2)_{r_c\to\infty}=\frac{1}{4\pi\kappa_w}\frac{\mu}{r^2}\cos\theta,\end{aligned} \tag{A2}$$

where μ is the magnitude of the dipole. From the boundary conditions, the potential and electric field in the polymer are determined as

$$\begin{aligned}&\phi_1=\frac{1}{4\pi\kappa_w}\frac{3}{2\kappa_p/\kappa_w+1}\frac{\mu}{r^2}\cos\theta,\\ &\mathbf{E}(\mathbf{r})=-\frac{1}{4\pi\kappa_w}\frac{3}{2\kappa_p/\kappa_w+1}\left[\frac{\boldsymbol{\mu}}{r^3}-\frac{3(\boldsymbol{\mu}\cdot\mathbf{r})\mathbf{r}}{r^5}\right].\end{aligned} \tag{A3}$$

APPENDIX B: THE EFFECTIVE DIELECTRIC CONSTANT OF COMPOSITES

The swollen Nafion can be regarded as a two-phase composite system, with hydrophilic clusters embedded in a hydrophobic polymer-backbone continuum. The effective dielectric constant of the two-phase composite can be expressed rigorously as[10]

$$\boldsymbol{\kappa}_e=(1-c)\boldsymbol{\kappa}_1\mathbf{A}_1+c\boldsymbol{\kappa}_2\mathbf{A}_2, \tag{B1}$$

where $\boldsymbol{\kappa}_1$ and $\boldsymbol{\kappa}_2$ are the dielectric tensors of phase 1 and 2, $\mathbf{A}_1$ and $\mathbf{A}_2$ are the corresponding field concentration tensors, and c is the volume fraction of phase 2. The concentration tensors are defined by

$$\langle\mathbf{E}_1\rangle=\mathbf{A}_1\mathbf{E}^0,\ \ \langle\mathbf{E}_2\rangle=\mathbf{A}_2\mathbf{E}^0,\ \ (1-c)\mathbf{A}_1+c\mathbf{A}_2=\mathbf{I}, \tag{B2}$$

where $\langle\mathbf{E}\rangle$ denotes the volume average of $\mathbf{E}$, $\mathbf{E}^0$ is the electric field applied at the boundary, and $\mathbf{I}$ is the second-order unit tensor. It is clear that the determination of the effective dielectric constant depends on the determination of the concentration tensor. To do this, we adopt the Mori-Tanaka mean field approach,[31] assuming that the average field, $\langle\mathbf{E}_2\rangle$, in phase 2, is equal to the average field in a single cluster embedded in an infinite matrix subjected to an external field equal to the yet-unknown average field, $\langle\mathbf{E}_1\rangle$, in phase 1,

$$\mathbf{E}_2=\mathbf{A}_2^{\mathrm{dil}}\mathbf{E}_1,\ \ \mathbf{A}_2^{\mathrm{dil}}=[\mathbf{I}+\mathbf{S}\boldsymbol{\kappa}_1^{-1}(\boldsymbol{\kappa}_2-\boldsymbol{\kappa}_1)]^{-1}, \tag{B3}$$

where $\mathbf{A}^{\mathrm{dil}}$ is a concentration tensor for the dilute distribution of clusters (i.e., no interaction with other clusters), and can be determined exactly, using Eshelby's equivalent-inclusion concept.[32] In Eq. (B3), $\mathbf{S}$ is the dielectric Eshelby tensor. For a spherical inclusion embedded in an isotropic matrix,[33] $S_{11}=S_{22}=S_{33}=\frac{1}{3}$. From Eqs. (B2) and (B3), we have

$$\mathbf{A}_2=\mathbf{A}_2^{\mathrm{dil}}[(1-c)\mathbf{I}+c\mathbf{A}_2^{\mathrm{dil}}]^{-1}. \tag{B4}$$

From Eqs. (B1) to (B4), after some manipulation, we finally obtain

$$\kappa_e=\frac{\kappa_1+\kappa_2-c(\kappa_1-\kappa_2)}{\kappa_1+\kappa_2+c(\kappa_1-\kappa_2)}\kappa_1, \tag{B5}$$

for isotropic constituents and composites.

[1] P. Millet, M. Pineri, and R. Durand, J. Appl. Electrochem. **19**, 162 (1989).
[2] H. Takenaka, E. Torikai, Y. Kawami, and N. Wakabayashi, Int. J. Hydrogen Energy **7**, 397 (1982).
[3] K. Oguro, K. Asaka, and H. Takenaka, Proceedings of 4th International Symposium on Micro Machine and Human Science at Nagoya, 1993, p. 39.
[4] K. Sadeghipour, R. Salomon, and S. Neogi, Smart Mater. Struct. **1**, 172 (1992).
[5] M. Shahinpoor, Smart Mater. Struct. **1**, 91 (1992).
[6] S. Sewa, K. Onishi, K. Asaka, N. Fujiwara, and K. Oguro, Proceedings MEMS 98. IEEE. Eleventh Annual International Workshop on Micro Electro Mechanical Systems. An Investigation of Micro Structures, Sensors, Actuators, Machines and Systems, 1998, p. 148.
[7] W. Kuhn, Experientia **5**, 318 (1949).
[8] W. Kuhn, B. Hargitay, A. Katchalsky, and H. Eisenberg, Nature (London) **165**, 514 (1950).
[9] Y. Osada and J. Gong, Prog. Polym. Sci. **18**, 187 (1993).
[10] S. Nemat-Nasser and M. Hori, *Micromechanics: Overall Properties of Heterogeneous Materials*, 2nd ed. (Elsevier, North-Holland, Amsterdam, 1999).
[11] P. Millet, R. Durand, E. Dartyge, G. Tourillon, and A. Fontaine, J. Electrochem. Soc. **140**, 1373 (1993).

[12] A. Eisenberg, Macromolecules **3**, 147 (1970).
[13] T. D. Gierke, G. E. Munn, and F. C. Wilson, J. Polym. Sci., Polym. Phys. Ed. **19**, 1687 (1981).
[14] W. A. Forsman, Macromolecules **15**, 1032 (1982).
[15] N. Lakshminarayanaiah, *Transport Phenomena in Membranes* (Academic, New York, 1969).
[16] M. A. Biot, J. Appl. Phys. **26**, 182 (1955).
[17] P. E. Grimshaw, J. H. Nussbaum, A. J. Grodzinsky, and M. L. Yarmush, J. Chem. Phys. **93**, 4462 (1990).
[18] W. Y. Hsu and T. D. Gierke, Macromolecules **15**, 101 (1982).
[19] T. Xue, J. S. Trent, and K. Osseo-Asare, J. Membr. Sci. **45**, 261 (1989).
[20] E. M. Lee, R. K. Thomas, A. N. Burgess, D. Y. Barnes, A. K. Soper, and A. R. Rennil, Macromolecules **25**, 3106 (1992).
[21] K. A. Mauritz, J. Macromol. Sci. Rev. Macromol. Chem. C **28**, 65 (1988).
[22] C. Heitner-Wirguin, J. Membr. Sci. **120**, 1 (1996).
[23] A. E. H. Love, *A Treatise on the Mathematical Theory of Elasticity* (Dover, New York, 1944).
[24] W. B. Cheston, *Elementary Theory of Electric and Magnetic Fields* (Wiley, New York, 1964).
[25] A. Narebska, S. Koter, and W. Kujawski, J. Membr. Sci. **25**, 153 (1985).
[26] K. A. Mauritz and C. E. Rogers, Macromolecules **18**, 483 (1985).
[27] R. Kanno, S. Tadokoro, T. Takamori, M. Hattori, and K. Oguro, Proceedings of the 1996 IEEE International Conference on Robotics and Automation, 1996, p. 219.
[28] M. Shahinpoor, Y. Bar-Cohen, J. O. Simpson, and J. Smith, Smart Mater. Struct. **7**, 15 (1998).
[29] M. Mojarrad and M. Shahinpoor, Proc. SPIE **3042**, 52 (1997).
[30] C. J. F. Bottcher, *Theory of Electric Polarization* (Elsevier, Netherlands, 1952).
[31] T. Mori and Y. Tanaka, Acta Metall. **21**, 571 (1973).
[32] J. D. Eshelby, Proc. R. Soc. London, Ser. A **241**, 376 (1957).
[33] M. Taya and R. J. Arsenault, *Metal Matrix Composites, Thermomechanical Behavior*, Pergamon, New York, 1989.